Total Synthesis of Dynobactin A

Fabian Schneider,† Yinliang Guo,† You-Chen Lin,† Kelly J. Eberle, Debora Chiodi, Jonathan A. Greene, Chenxin Lu, and Phil S. Baran*

Department of Chemistry, Scripps Research, 10550 North Torrey Pines Road, La Jolla, CA 92037, United States.

Supporting Information Placeholder

ABSTRACT: The first total synthesis of the potent antimicrobial agent dynobactin A is disclosed. This synthesis capitalizes on the hidden symmetry present in this complex decapeptide by enlisting an aziridine ring opening strategy to access β-branched amino acids. Featuring a number of unique maneuvers to navigate inherently sensitive and epimerizable functional groups, this convergent approach proceeds in only 14 steps (LLS) from commercial materials and should facilitate the synthesis of numerous analogs for medicinal chemistry studies.

In the face of growing antibiotic resistance, the search for novel antibiotics has become a global health priority,[1] specifically in regard to gram-negative bacteria, which possess an outer membrane that is highly resistant to penetration by most antibiotics.[2-3] Darobactin A[4] (**1**, Figure 1) and Dynobactin A[5-6] (**2**, Figure 1) are recently discovered natural products that show promising potent antibacterial properties against gram-negative pathogens, as well as low cytotoxicity. Adding further intrigue and promise to this class of antibiotics is its apparent ability to evade bacterial resistance through mutation.[7] As such, the bactericidal activity of these natural products is of great interest and importance to the scientific community. Both **1** and **2** target BamA, a bacterial insertase within the BAM complex[8-9] that facilitates folding and insertion of outer membrane proteins in gram-negative bacteria.[10-16] However, **2**, a decapeptide featuring two linked macrocycles, stands structurally distinct from its BamA-targeting counterpart **1**. The unfused bicyclic structure possibly endows dynobactin A with flexibility and additional ionizable sites, resulting in a water solubility that exceeds that of **1** by more than 20-fold.[5] The synthetic challenge posed by **1** was addressed concurrently last year by two separate groups.[17-18] **2** encompasses several unique structural elements, including a C–C bond formed between C6 of the tryptophan residue and the β-carbon of the asparagine (C21), as well as a rare N-C linkage bridging the imidazole of histidine and β-carbon (C39) of the tyrosine unit. These intriguing structural complexities render **2** an exciting subject for synthetic pursuit. Yet, the intricate structure of **2** along with its natural scarcity pose a challenge to conventional (semi)synthetic approaches. This synthesis of **2** is concise considering its complexity, due to the recognition of a hidden strategic symmetry wherein parallel aziridine openings forge the challenging β-aryl disubstituted amino acids found in **2** prior to convergent assembly. In this Communication, the first total synthesis of **2** is disclosed, potentially enabling a deeper exploration of this promising natural product family.

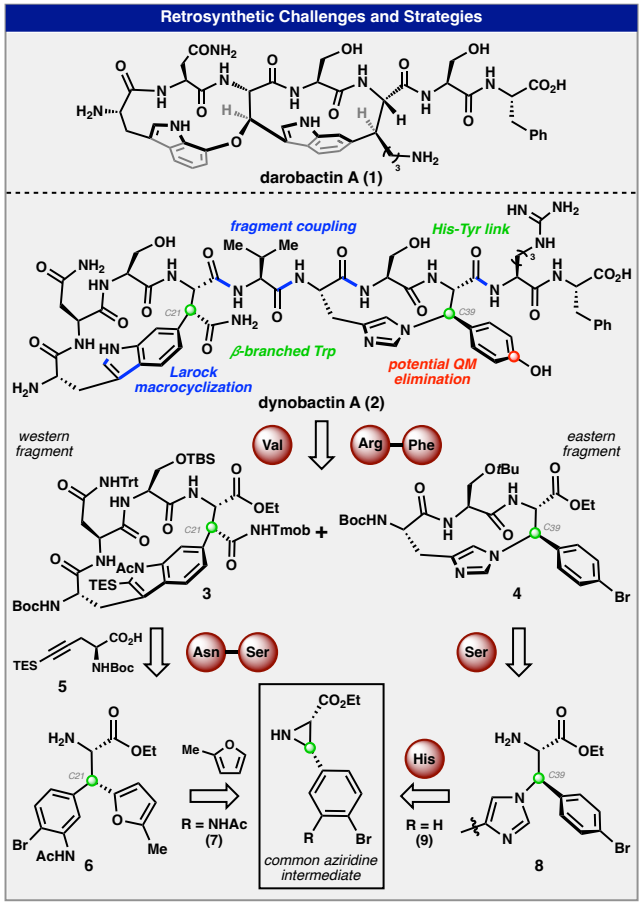

Figure 1. Darobactin A (**1**) and Dynobactin A (**2**): Retrosynthetic strategies

Retrosynthetically, **2** (Figure 1) was envisioned to arise from a C-terminal Arg-Phe dipeptide unit and appendage of the two macrolactam subunits to the central valine residue, resulting in two fragments comprising a 17-membered (**3**, western fragment) and 12-membered (**4**, eastern fragment) macrolactam, respectively. Our lab recently published a modular, atroposelective synthetic route to **1**.[17] While distinct in overall structure, the shared features of **1** and the western macrocycle of **2** suggested that the macrocyclization strategy employed in that synthesis may also be applicable herein to obtain **3**. In order to generate the western fragment via Larock indole synthesis, the framework would be constructed from an asparagine unit, serine unit, alkyne fragment **5**, and the requisite aniline in the

form of a β-aryl asparagine. **4** was proposed to be constructed via macrocyclization along the His-Ser peptide bond. The overall synthetic strategy was centered around the construction of the β-branched amino acid units which are characteristic of the biosynthetic origin of **2** as a RiPP natural product. Key to the execution of this plan was that the branched AAs **6** and **8** could both be derived using the same nucleophilic ring-opening strategy upon aziridines **7** and **9**, respectively (*vide infra*).

Extensive route scouting was conducted to understand the basic reactivity and workable strategies for such systems (Figure 2). Initially, the synthesis of the β-branched Asn fragment of the western fragment **3** was pursed by an epoxide opening reaction with enolate-type nucleophiles (Figure 2a, strategy A). Although the primary alcohol obtained proved competent for construction of the western fragment, all attempts for its late-stage conversion to the corresponding primary amide were hampered by extensive epimerization of the benzylic α-carbonyl stereocenter (see SI). This issue necessitated the introduction of a non-epimerizable surrogate for the primary amide. For construction of the β-branched tyrosine moiety of the eastern fragment **4**, a broad range of strategies were evaluated (Figure 2, strategies B–D). Linkages of this type are extremely rare and notoriously difficult to obtain synthetically. Indeed, no successful strategy has been uncovered to date.[19-20] Attempted nucleophilic substitution reactions under either neutral, anionic or halogenide/Ag^+-facilitated conditions led consistently to either formation of the corresponding unsaturated dehydro-amino acid or decomposition of the substrates (Figure 2b, strategy B, see SI). Attempts to utilize addition of the histidine imidazole to an acyl aziridine moiety were hampered by the electronic nature of the acyclic twisted amide such obtained (Figure 2b, strategy C). The lack of n_N to $\pi^*_{C=O}$ conjugation of this moiety lead to facile epimerization of the adjacent serine α-stereocenter even under mild conditions. Besides this, cleavage of the aziridine amide by nucleophiles was observed as a dominant side reaction (see SI). Further, a potentially biomimetic intramolecular cyclization by addition of the histidine imidazole to the corresponding tyrosine-derived quinone methide was considered (Figure 2b, strategy D). However, this approach led mostly to either decomposition or tautomerization to the corresponding dehydro-tyrosine (see SI). In addition to the approaches described, several other strategies were

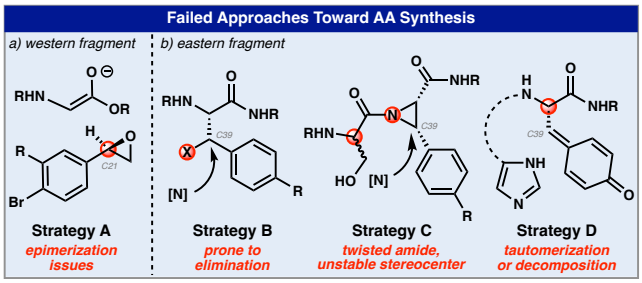

evaluated for β-amino acid synthesis; see SI for further detail.

Figure 2. Synthetic strategies towards β-branched amino acids

A breakthrough was reached upon recognition that the β-branched amino acid motifs for both **3** and **4** could, in principle, be derived from aziridine ring openings (Figure 1). While addition to aziridines has previously been demonstrated as a useful strategy for the synthesis of β-branched amino acids,[21] very few examples exist for comparable additions to α-carbonyl, β-aryl aziridines as was necessitated in the case of **2**. In general, addition to aziridines requires the use of electron-withdrawing *N*-activators (such as tosyl or nosyl protecting groups), which could potentially introduce further synthetic issues. For instance, cleavage of *N*-tosyl is incompatible with use of an aryl bromide,[22-23] preliminary experiments indicated difficulties in controlling the reactivity for *N*-nosyl,[24] and rearrangement is a known issue for carbamate-based protecting groups.[25-26] For these reasons, a more efficient approach was developed based on direct addition into free-NH aziridines. The β-branched motif of **4** could thus be traced back to addition of histidine into chiral aziridine **9** to forge the N-C39 bond of **2**. To mitigate the risk of imidazole eliminating from tyrosine to form the corresponding *para*-quinone methide (QM) (Figure 1, highlighted in red), bromide was chosen as a stable surrogate for hydroxyl group of the natural tyrosine with the intention to introduce the requisite phenol moiety at a late stage. The synthesis of the western fragment **3** branched tryptophan-asparagine motif (Figure 1, highlighted in green) was envisioned in the same fashion by addition of 2-methyl furan into the corresponding aziridine **7**. In this case, furan acts as an epimerization-proof synthetic precursor to the primary asparagine amide, to be unveiled towards the end of the synthesis. With a strategy in hand to address the challenge of synthesizing the β-branched amino acids **6** and **7**, our attention next turned to construction of the two macrocycles and final assembly of **2**.

The synthesis of **2** is outlined in Scheme 1. To construct the eastern fragment **4**, enantioenriched **9** (93:7 er) was prepared in good yield on multigram-scale in two steps, leveraging the multicomponent asymmetric aziridination developed by Wulff group (see SI for experimental detail).[27] With ample quantities of free aziridine **9** in hand, a stereo- and regio- selective aziridine opening reaction was conducted using histidine derivative **11** as a nucleophile under acidic conditions. This reaction was subjected to extensive optimization (see Scheme 1 Table 1 and SI for further detail) and showed a pronounced solvent dependence, wherein the use of trifluoroethanol (TFE) was found to be critical. The role of TFE in this reaction may be rationalized by a unique combination of high polarity, low nucleophilicity, and the ability to form H-bonding adducts with donor functionalities, aiding in the ring opening reaction of the aziridine.[28-29] The major side reaction pathway under optimized conditions was identified as dimer formation by competing nucleophilic attack of the aziridine. The ratio between the desired product and dimer is critically influenced by the protonation equilibrium of the aziridine and nucleophile (see SI for a comparison of nucleophiles with varying pK_a). The direct reaction between His **10** and aziridine **9** was hampered by extensive dimer formation due to an insufficient pK_a difference. In comparison, utilization of less basic 5-Br-His **11** led to a subtle shift in protonation equilibrium resulting in reduced dimer formation to give the desired aziridine addition in 41–65% yield depending upon the equivalents of His **11** utilized. Subsequent reductive cleavage of the bromide under acidic conditions using Zn/AcOH proceeded with excellent selectivity for the bromo-imidazole in nearly quantitative yield and enabled access to the key β-branched amino acid coupled product **8**. Subsequent steps included amide coupling with a protected serine residue to furnish cyclization precursor **12**, which was subjected to TBAF, resulting in simultaneous Fmoc and (trimethylsilyl)ethyl (TSE) deprotection. After screening a variety of activation reagents, the combination of PyAOP with HOAt was found to be the most effective conditions under which to forge the macrocycle to yield **4** in 54% yield over two steps.

The aziridine-based strategy outlined above could be leveraged again to forge the tryptophan-asparagine linkage. Thus, western fragment **3** was prepared by employing 2-methyl furan as a nucleophile onto aziridine **7**. The use of 2-methylfuran as a masked primary amide provided several advantages, notably avoiding undesired side reactions such as epimerization of the β-carbon and imide formation during carboxylic acid activation. The resulting ring-opened product **6** was enlisted directly in a one-pot amide

coupling with compound **13**. A subsequent Fmoc deprotection and amide coupling with alkyne **5** (Figure 1) yielded the cyclization precursor **14** in 56% yield over two steps. Borrowing from the strategy previously developed to access **1**,[17] a Larock macrocyclization was employed to form the 17-membered ring, providing **15** in 52% yield using a catalytic quantity of Pd. Due to the increased ring size of **15** relative to **1**, no atropisomers were observed for this macrocycle.[30] The protected primary amide functionality was then unveiled via furan oxidation using a Ru catalyst and subsequent aminolysis to afford the completed western fragment **3** in 41% yield. A number of different permutations were tested for the sequence of valine introduction, east-west-fragment coupling, and furan oxidation (an overview is given in Table 2 and in the SI). Approaches to undertake the oxidative cleavage of the furan late-stage after fragment coupling together the 8-mer or 10-mer peptide (with/without the Arg-Phe side chain, see Table 2 and SI) led only to decomposition of the substrate, presumably due to interference with the electron-rich imidazole moiety. Coupling of the valine residue to the western fragment **15** followed by oxidative cleavage of the furan/aminolysis, while successful on small scale, resulted in long reaction times (5 days) and diminished yields (< 20%) upon scaleup. In contrast, oxidative cleavage of the furan directly on intermediate **15** proceeded faster (12–24 h) and in higher yield and was thus chosen as the optimal order of operations for this sequence. The ethyl ester moiety of **15** was then hydrolyzed using trimethyltin hydroxide[31] to afford **16** and set the stage for the assembly of the decapeptide.

Following Boc deprotection with formic acid, eastern fragment **4** was coupled to the central valine residue to generate **17** in 48% yield. Trityl deprotection of **17** followed by coupling with western fragment **16** gave **18** in 56% yield. Remarkably, the fragment coupling on the C-terminus of the branched asparagine proceeded with no substantial aspartimide-related side reactions (e.g., deamination, dehydration, isomerization).[32] This fragment coupling strategy, conjoining both fragments as equally sized tetra-peptides, is the most convergent approach to the fragment coupling of the iterations evaluated (see Table 3). As mentioned above, fragment coupling attempts prior to furan oxidation were non-viable, given the sensitivity of late-stage intermediates to the oxidation conditions. Appendage of the valine unit to the western macrocycle followed by coupling of the eastern macrocycle was comparably successful. A potentially more convergent assembly of the decapeptide featuring introduction to the dipeptide Arg-Phe to the eastern fragment before east-west-fragment coupling was not successful (see Table 3). As such, **18** was subjected to ester hydrolysis and subsequent coupling with **19** to arrive at the decapeptide **20**. At this point, all that remained was conversion of the bromide to the requisite hydroxyl group, followed by global deprotection to complete the synthesis of **2**. The final transformations were accomplished in a one-pot procedure consisting of: (1) Miyaura borylation of the bromide with concomitant deprotection of acid-labile protecting groups, (2) oxidation of the resulting boronic acid to the phenol, (3) hydrogenolysis of the benzyl ester, and (4) removal of the final acetyl protecting group on the indole moiety. This final sequence provided **2** in 55% yield, with 14 steps LLS from commercially available starting materials. Synthetic **2** was found to be spectroscopically and chromatographically identical to an authentic sample of the natural product (see SI).

To summarize, a convergent total synthesis of **2** has been accomplished by leveraging hidden symmetry of the seemingly distinct eastern and western halves of the molecule. A unique (and perhaps general) strategy for the synthesis of β-branched amino acids that enlists simple N-H aziridine building blocks in either stereo- and regioselective C–C (western fragment) or N–C (eastern fragment) ring opening events enabled this plan. The strategic use of a furan and aryl bromide to shield the most sensitive parts of the final natural product are also noteworthy tactics. The modular approach to **2** should enable an extensive study of the SAR of this fascinating family of antibiotics.

Scheme 1. Total synthesis of dynobactin A[a]

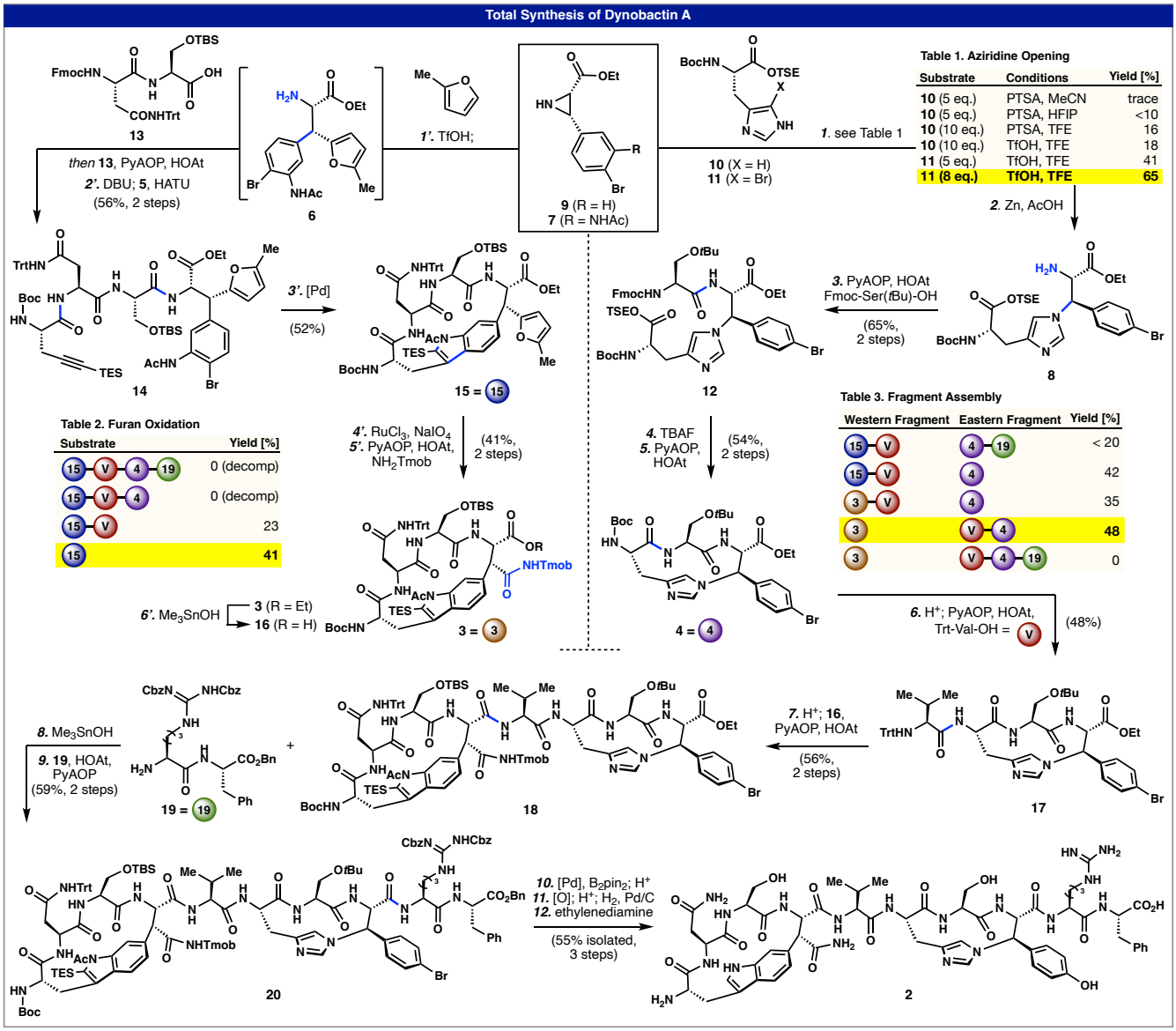

[a]Reagents and conditions. Eastern Fragment: (**1**) TfOH (2.2 equiv), TFE, 0 to 80 °C, 65%. (**2**) Zn (5.0 equiv), AcOH, rt. (**3**) Fmoc-Ser(*t*Bu)-OH (1.2 equiv), HOAt (1.5 equiv), PyAOP (1.2 equiv), DIPEA (3 equiv), DCM, rt, 65% over 2 steps. (**4**) TBAF (3.5 equiv), THF, 0 °C to rt. (**5**) PyAOP (1.1 equiv), HOAt (5 equiv), DIPEA (8 equiv), DMF, rt, 54% over 2 steps. Western Fragment: (**1'**) TfOH (80 mol%), methyl furan (24 equiv), TFE, -78°C to 38 °C; **13** (1.0 equiv), PyAOP (1.1 equiv), DIPEA (3.5 equiv), DMF, rt, 73%. (**2'**) DBU (1.85 equiv), DCM, rt; **5** (1.2 equiv), PyAOP (1.2 equiv), DIPEA (3.80 equiv), DMF/DCM 1:1, rt, 56%. (**3'**) $Pd(PtBu_3)_2$ (30 mol%), DIPEA (50 equiv), dioxane, 95 °C, 52%. (**4'**) $RuCl_3$ (25 mol%), $NaIO_4$ (127 equiv), $NaHCO_3$ (232 equiv) hexane/ EtOAc/H_2O 1:2:2, rt. (**5'**) Tmob-NH_2 (5.0 equiv), PyAOP (1.1 equiv), HOAt (5.0 equiv), DIPEA (10 equiv), DCM, rt, 41% over 2 steps. (**6'**) Me_3SnOH (16 equiv), DCE, 80 °C. Final Assembly sequence: (**6**) formic acid/DCM 1:1, 40 °C; Trt-Val-OH (3.0 equiv), PyAOP (3.0 equiv), HOAt (5.0 equiv), DIPEA (10 equiv), DCM/DMF 4:1, rt, 48%. (**7**) MeOH/formic acid 5:1, rt; **16** (1.5 equiv), PyAOP (1.2 equiv), HOAt (5.0 equiv), DIPEA (8.0 equiv), DCM/DMF 4:1, rt, 56% over 2 steps. (**8**) Me_3SnOH (16 equiv), DCE, 80 °C. (**9**) **19** (3.0 equiv), PyAOP (1.2 equiv.), HOAt (5 equiv), DIPEA (10 equiv), DCM/DMF 4:1, rt, 59%, 2 steps. (**10**) B_2pin_2 (20 equiv), $Pd_2(dba)_3$ (50 mol%), XPhos (2.0 equiv), KOAc (20 equiv), dioxane, rt; TFA, Et_3SiH, DCM, rt. (**11**) $NaBO_3 \cdot 4\ H_2O$ (20 equiv), H_2O/THF, rt; HCl in dioxane, rt; H_2 (*g*), Pd/C (4.0 equiv), MeOH, rt. (**12**) ethylenediamine, MeOH, rt, 55% over the final three step sequence.

ASSOCIATED CONTENT

Supporting Information. Experimental procedures, analytical data (^1H and ^{13}C NMR, MS) for all new compounds as well as optimization tables.

AUTHOR INFORMATION

Corresponding Authors

E-mail: pbaran@scripps.edu (P.S.B.).

Author Contributions

†F.S., Y. G., and Y. C. L. contributed equally to this work.

Notes

The authors declare no competing financial interest.

ACKNOWLEDGMENTS

Financial support for this work was provided by NIGMS (GM-118176) and a Feodor-Lynen fellowship to F.S. by the Alexander von Humboldt Foundation. We are grateful to Dr. G. J. A. Kroon, Dr. D.-H. Huang and Dr. L. Pasternack (Scripps Research) for NMR spectroscopic assistance, Dr. J. Chen, Ms. B. Sanchez, and Ms. Q. N. Wong (Scripps Research) for analytical support. Prof. K. Lewis (Northeastern University) for providing a sample of authentic dynobactin A. Dr. M. Sofiadis, Dr. M. Nassir, Dr. M. Costantini, Dr. G. Laudadio, B. Nißl, A. Pollatos, and D. Xu for insightful discussions.

REFERENCES

(1) Tacconelli, E.; Carrara, E.; Savoldi, A.; Harbarth, S.; Mendelson, M.; Monnet, D. L.; Pulcini, C.; Kahlmeter, G.; Kluytmans, J.; Carmeli, Y.; Ouellette, M.; Outterson, K.; Patel, J.; Cavaleri, M.; Cox, E. M.; Houchens, C. R.; Grayson, M. L.; Hansen, P.; Singh, N.; Theuretzbacher, U.; Magrini, N.; Workin, W. P. P. L., Discovery, research, and development of new antibiotics: the WHO priority list of antibiotic-resistant bacteria and tuberculosis. *Lancet Infect. Dis.* **2018**, *18,* 318–327.
(2) Li, X. Z.; Nikaido, H., Efflux-mediated drug resistance in bacteria. *Drugs* **2004**, *64,* 159–204.
(3) Lomovskaya, O.; Lewis, K., Emr, an Escherichia-Coli Locus for Multidrug Resistance. *Proc. Natl. Acad. Sci. U.S.A.* **1992**, *89,* 8938–8942.
(4) Imai, Y.; Meyer, K. J.; Iinishi, A.; Favre-Godal, Q.; Green, R.; Manuse, S.; Caboni, M.; Mori, M.; Niles, S.; Ghiglieri, M.; Honrao, C.; Ma, X. Y.; Guo, J. J.; Makriyannis, A.; Linares-Otoya, L.; Boehringer, N.; Wuisan, Z. G.; Kaur, H.; Wu, R.; Mateus, A.; Typas, A.; Savitski, M. M.; Espinoza, J. L.; O'Rourke, A.; Nelson, K. E.; Hiller, S.; Noinaj, N.; Schäberle, T. F.; D'Onofrio, A.; Lewis, K., A new antibiotic selectively kills Gram-negative pathogens. *Nature* **2019**, *576,* 459–464.
(5) Miller, R. D.; Iinishi, A.; Modaresi, S. M.; Yoo, B. K.; Curtis, T. D.; Lariviere, P. J.; Liang, L.; Son, S.; Nicolau, S.; Bargabos, R.; Morrissette, M.; Gates, M. F.; Pitt, N.; Jakob, R. P.; Rath, P.; Maier, T.; Malyutin, A. G.; Kaiser, J. T.; Niles, S.; Karavas, B.; Ghiglieri, M.; Bowman, S. E. J.; Rees, D. C.; Hiller, S.; Lewis, K., Computational identification of a systemic antibiotic for gram-negative bacteria. *Nat. Microbiol.* **2022**, *7,* 1661–1672.
(6) Munoz, K. A.; Hergenrother, P. J., Computational discovery of dynobactin antibiotics. *Nat. Microbiol.* **2022**, *7,* 1512–1513.
(7) Kaur, H.; Jakob, R. P.; Marzinek, J. K.; Green, R.; Imai, Y.; Bolla, J. R.; Agustoni, E.; Robinson, C. V.; Bond, P. J.; Lewis, K.; Maier, T.; Hiller, S., The antibiotic darobactin mimics a beta-strand to inhibit outer membrane insertase. *Nature* **2021**, *593,* 125–129.
(8) Knowles, T. J.; Scott-Tucker, A.; Overduin, M.; Henderson, I. R., Membrane protein architects: the role of the BAM complex in outer membrane protein assembly. *Nat. Rev. Microbiol.* **2009**, *7,* 206–214.
(9) Noinaj, N.; Rollauer, S. E.; Buchanan, S. K., The beta-barrel membrane protein insertase machinery from Gram-negative bacteria. *Curr. Opin. Struct. Biol.* **2015**, *31,* 35–42.
(10) Doyle, M. T.; Bernstein, H. D., Bacterial outer membrane proteins assemble via asymmetric interactions with the BamA beta-barrel. *Nat. Commun.* **2019**, *10,* 3358.
(11) Lee, J.; Tomasek, D.; Santos, T. M.; May, M. D.; Meuskens, I.; Kahne, D., Formation of a beta-barrel membrane protein is catalyzed by the interior surface of the assembly machine protein BamA. *eLife* **2019**, *8*.
(12) Iadanza, M. G.; Higgins, A. J.; Schiffrin, B.; Calabrese, A. N.; Brockwell, D. J.; Ashcroft, A. E.; Radford, S. E.; Ranson, N. A., Lateral opening in the intact beta-barrel assembly machinery captured by cryo-EM. *Nat. Commun.* **2016**, *7,* 12865.
(13) Konovalova, A.; Kahne, D. E.; Silhavy, T. J., Outer Membrane Biogenesis. *Annu. Rev. Microbiol.* **2017**, *71,* 539–556.
(14) Gu, Y.; Li, H.; Dong, H.; Zeng, Y.; Zhang, Z.; Paterson, N. G.; Stansfeld, P. J.; Wang, Z.; Zhang, Y.; Wang, W.; Dong, C., Structural basis of outer membrane protein insertion by the BAM complex. *Nature* **2016**, *531,* 64–69.
(15) Noinaj, N.; Kuszak, A. J.; Gumbart, J. C.; Lukacik, P.; Chang, H.; Easley, N. C.; Lithgow, T.; Buchanan, S. K., Structural insight into the biogenesis of beta-barrel membrane proteins. *Nature* **2013**, *501,* 385–390.
(16) Bakelar, J.; Buchanan, S. K.; Noinaj, N., The structure of the beta-barrel assembly machinery complex. *Science* **2016**, *351,* 180–186.
(17) Lin, Y. C.; Schneider, F.; Eberle, K. J.; Chiodi, D.; Nakamura, H.; Reisberg, S. H.; Chen, J. S.; Saito, M.; Baran, P. S., Atroposelective Total Synthesis of Darobactin A. *J. Am. Chem. Soc.* **2022**, *144,* 14458–14462.
(18) Nesic, M.; Ryffel, D. B.; Maturano, J.; Shevlin, M.; Pollack, S. R.; Gauthier, D. R., Jr.; Trigo-Mourino, P.; Zhang, L. K.; Schultz, D. M.; McCabe Dunn, J. M.; Campeau, L. C.; Patel, N. R.; Petrone, D. A.; Sarlah, D., Total Synthesis of Darobactin A. *J. Am. Chem. Soc.* **2022**, *144,* 14026–14030.
(19) Bravo, J.; Fita, I.; Ferrer, J. C.; Ens, W.; Hillar, A.; Switala, J.; Loewen, P. C., Identification of a novel bond between a histidine

and the essential tyrosine in catalase HPII of Escherichia coli. *Protein Sci.* **1997**, *6,* 1016–1023.
(20) Li, Y.; Ma, Y.; Xia, Y.; Zhang, T.; Sun, S.; Gao, J.; Yao, H.; Wang, H., Discovery and biosynthesis of tricyclic copper-binding ribosomal peptides containing histidine-to-butyrine crosslinks. *Nat. Commun.* **2023**, *14,* 2944.
(21) Michaux, J.; Niel, G.; Campagne, J. M., Stereocontrolled routes to beta,beta'-disubstituted alpha-amino acids. *Chem. Soc. Rev.* **2009**, *38,* 2093–2116.
(22) MacKenzie, I. A.; Wang, L. F.; Onuska, N. P. R.; Williams, O. F.; Begam, K.; Moran, A. M.; Dunietz, B. D.; Nicewicz, D. A., Discovery and characterization of an acridine radical photoreductant. *Nature* **2020**, *580,* 76–80.
(23) As the reduction potential range for aryl bromides (Ep/2 = -1.6 (*p*-CF_3ArBr) to –2.90 V (*p*-OMeArBr) vs SCE) and tosyl sulfonamides (Ep/2 = –2.01 (aniline) to -2.6 V (N-Ts-pyrrolidine) vs SCE) shows substantial overlap, differentiation for reductive cleavage of tosyl protected amines and electronically neutral aryl bromides is expected to be tedious.
(24) Preliminary experiments utilizing N-nosyl-aziridine analogues of intermediates 7 and 9 tended to result in complex mixtures, likely as a result of the high intrinsic reactivity of these substrates in case of aryl aziridines.
(25) Hu, X. E., Nucleophilic ring opening of aziridines. *Tetrahedron* **2004**, *60,* 2701–2743.
(26) Tirotta, I.; Fifer, N. L.; Eakins, J.; Hutton, C. A., Synthesis of tryptophans by Lewis acid promoted ring-opening of aziridine-2-carboxylates: optimization of protecting group and Lewis acid. *Tetrahedron Lett.* **2013**, *54,* 618–620.
(27) Gupta, A. K.; Mukherjee, M.; Wulff, W. D., Multicomponent catalytic asymmetric aziridination of aldehydes. *Org. Lett.* **2011**, *13,* 5866–5869.
(28) Sherry, A. D.; Purcell, K. F., Linear Enthalpy-Spectral Shift Correlations for 2,2,2-Trifluoroethanol. *J. Phys. Chem.* **1970**, *74,* 3535–3543.
(29) Colomer, I.; Chamberlain, A. E. R.; Haughey, M. B.; Donohoe, T. J., Hexafluoroisopropanol as a highly versatile solvent. *Nat. Rev. Chem.* **2017**, *1,* 0088.
(30) Breazzano, S. P.; Poudel, Y. B.; Boger, D. L., A Pd(0)-Mediated Indole (Macro)cyclization Reaction. *J. Am. Chem. Soc.* **2013**, *135,* 1600–1606.
(31) Nicolaou, K. C.; Estrada, A. A.; Zak, M.; Lee, S. H.; Safina, B. S., A mild and selective method for the hydrolysis of esters with trimethyltin hydroxide. *Angew. Chem., Int. Ed.* **2005**, *44,* 1378–1382.
(32) Neumann, K.; Farnung, J.; Baldauf, S.; Bode, J. W., Prevention of aspartimide formation during peptide synthesis using cyanosulfurylides as carboxylic acid-protecting groups. *Nat. Commun.* **2020**, *11,* 982.